Liquid Crystals
Publication details, including instructions for authors and subscription information:
http://www.informaworld.com/smpp/title~content=t713926090

Horizontal chevron configurations in ferroelectric liquid crystal cells induced by high electric fields

I. Dierking[a]; F. Gießelmann[a]; J. Schacht[a]; P. Zugenmaier[a]
[a] Institut für Physikalische Chemie der TU Clausthal, Clausthal-Zellerfeld, Germany

To cite this Article Dierking, I. , Gießelmann, F. , Schacht, J. and Zugenmaier, P.(1995) 'Horizontal chevron configurations in ferroelectric liquid crystal cells induced by high electric fields', Liquid Crystals, 19: 2, 179 — 187
To link to this Article: DOI: 10.1080/02678299508031967
URL: http://dx.doi.org/10.1080/02678299508031967

LIQUID CRYSTALS, 1995, VOL. 19, NO. 2, 179–187

Horizontal chevron configurations in ferroelectric liquid crystal cells induced by high electric fields†

by I. DIERKING*, F. GIEßELMANN, J. SCHACHT and P. ZUGENMAIER
Institut für Physikalische Chemie der TU Clausthal, Arnold-Sommerfeld-Str. 4, D-38678 Clausthal-Zellerfeld, Germany

(*Received 16 January 1995; accepted 16 February 1995*)

Application of a high electric field to a S_C^* ferroelectric liquid crystal cell may cause the formation of horizontal chevron configurations with the smectic layers tilted by the amount of the chevron angle (in the case of the present investigation equal to the director tilt angle) with respect to the normal to the rubbing direction of the cell substrates. The layer structure resembles that of the well-known vertical chevron configuration, but in the plane of the substrate instead of perpendicular to it, and is similar to that recently reported for the stripe-shaped texture. Between crossed polarizers, the two domain types *appear* to switch in opposite directions when an a.c. electric field is applied. The temperature dependence of the observation of horizontal chevron structures was investigated and an explanation is proposed analogous to that for the stripe texture model.

1. Introduction

A variety of director configurations can be observed in S_C^* ferroelectric liquid crystals, depending on anchoring strength with the substrate and geometry of the sample. In thick samples, prepared on a glass slide without orientation layers, natural textures appear, as for example the well-known fan-shaped texture with the fans modulated by equidistant disclination lines, due to a helical director configuration of the S_C^* phase [1, 2]. These line textures may also be observed in LC cells with a well-defined cell gap and orientation layers, depending on the value of the S_C^* pitch [3]. If the cell gap is of the order of magnitude or smaller than the S_C^* pitch, the helix is elastically unwound by surface effects and a so-called 'surface stabilized ferroelectric liquid crystal' (SSFLC) geometry is obtained [3]. In the simplest case, a structure is observed in which the smectic layers are arranged almost perpendicular to the substrate plane and to the rubbing direction of the orientational layers with the *molecules* tilted with respect to the layer normal—the so-called bookshelf geometry (see figure 1 (*a*)). Due to anchoring effects at the substrate, usually a structure is observed with the *layers* tilted with respect to the substrate normal. This produces a smectic layer configuration, which has become known as the vertical chevron geometry [4–7], when the surfaces are rubbed in parallel directions (see figure 1 (*c*)), or simply tilted layers when they are rubbed antiparallel (see figure 1 (*b*)).

We have observed an electric field induced layer configuration, which resembles that of a chevron being turned by 90°, such that the smectic layers are tilted with respect to the normal of the rubbing direction by the amount of the chevron angle (equal to the director tilt angle) in the plane of the substrate, in contrast to the well-known vertical chevron geometry, where the smectic layers are tilted with respect to the substrate normal (see figure 2). Application of a high electric field to the LC cell results in the formation of two domain types, which seem to switch in an opposite sense, when viewed between crossed polarizers. The formation of the two domain types is analogous to observations by Patel *et al.* [8, 9], although the applied conditions were quite different. A similar

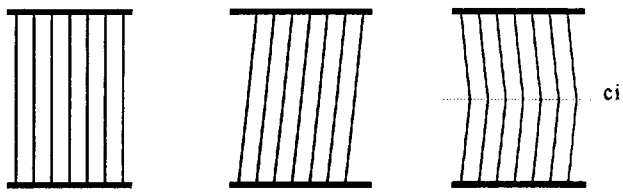

Figure 1. Schematic representation of different layer configurations in SSFLC cells: (*a*) the ideal bookshelf geometry, (*b*) the tilted layer geometry, usually observed in antiparallel rubbed LC cells and (*c*) the vertical chevron geometry with the chevron interface (ci), usually observed in parallel rubbed LC cells.

* Author for correspondence.

† Presented in part at the 10th International Conference on Textures of Materials, 20–24 September, 1993, Clausthal, Germany.

0267–8292/95 $10·00

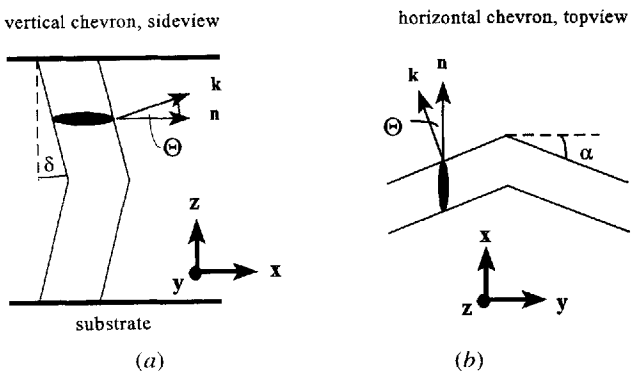

Figure 2. Schematic representation of the chevron layer configurations: (*a*) vertical chevron as a side view and (*b*) horizontal chevron as a top view of the cell. Nomenclature used: director **n**, layer normal **k**, rubbing direction **x**, direction of light propagation **z**, tilt angle θ, vertical chevron layer angle δ and horizontal chevron layer angle α.

behaviour was also observed by Andersson *et al.* [10], when a field induced N*–S_C^* transition was investigated. In the smectic A* phase, an analogous effect was observed for induced tilt angles [11]. The temperature dependence of this effect was investigated and the director- and layer-configuration verified by texture observation of different samples and investigations by an optical method discussed in detail below. The nomenclature used is schematically depicted in figure 2.

2. Experimental

Polarizing microscopic investigations were performed with an Olympus BH-2 microscope, equipped with a Mettler FP 52 hot stage and a Mettler FP 5 temperature controller. The effect of electric field induced domains was studied on two compounds. A commercially available epoxide [12, 13] (4-[(*S*,*S*)-2,3-epoxyhexyloxy]phenyl 4-decyloxybenzoate, abbreviated as EPHDBPE) with the phase sequence [14]

I 95·7 N* (78·1 S_C^*) (57·2 S_C^*) (°C)

in LC cells (E.H.C. Co. Ltd.) with 6 µm cell gap, ITO electrodes and parallel rubbed polyimide orientation layers served as a sample with a helical S_C^* director configuration. As a non-helical, surface stabilized sample, 4-(2′(*R*)-2′-chloro-3′-methylbutyroyloxy)-4′-(4′-octyloxybenzoyloxy)bibenzyl [15–17] (abbreviated as D8) was studied using 4 µm LC cells, with ITO electrodes and parallel rubbed polyimide orientation layers; this compound exhibits the phase sequence

I 134·5 N* 129·4 TGB A* 129·2 S_A^* 125·6 S_C^* 92·9 S_J^* 83·7 S_F^* (°C).

Measurements of the optical director tilt angle and the rotational position of the layer normal were performed using a method analogous to that introduced by Bahr *et al.* [18]. The transmission of the polarization up- and down-states of the FLC cell is recorded as a function of the orientation of the cell between crossed polars (rotation angle φ). The transmissions of the up- and down-states are described by $\sin^2(2\varphi)$-functions which exhibit a phase shift of 2θ with respect to each other (see figure 3). The transmissions of the up- and down-states are equal at the intersection point of both curves, and the polarizer points along the smectic layer normal. Therefore, the rotation angle of the intersection point represents the orientation of the layer normal. The electric field, which is used to switch between the up- and down-states, has to be an a.c. electric field in order to avoid screening of the external electric field by ionic impurities in the S_C^* phase. An electric square wave field was applied with frequency $f = 200$ Hz and amplitude $E = 1$ MV m^{-1}. The rubbing direction **x** of the polyimide orientation layer of the cell coincides with a rotation angle of the hot stage of $\varphi = 0°$. The transmitted light intensities of the two stationary states *polarization up* $I_{up}(\varphi)$ and *polarization down* $I_{down}(\varphi)$ are recorded as a function of the rotation angle φ. The director tilt angle θ and the angular position of the layer normal **k** with respect to the rubbing direction **x** is determined as follows: the transmitted light intensities of the two stationary states between crossed polarizers are described by

$$I_{up} \sim \sin^2(2(\varphi + \delta_{up})) \qquad (1\,a)$$

and

$$I_{down} \sim \sin^2(2(\varphi + \delta_{down})) \qquad (1\,b)$$

where φ is the rotation angle of the sample in the plane of the substrate and δ_{up}, δ_{down} are the phase shifts of the curves

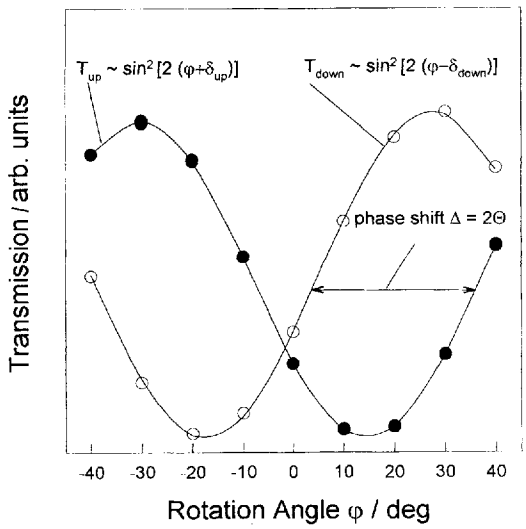

Figure 3. Illustration of the electro-optic method used to determine the director tilt angle θ and the orientation of the layer normal at the intersection.

for the two stationary states as compared to the $I(\varphi)$ curve in the S_A^* phase. The recorded intensities $I_{up,down}(\varphi)$ are normalized to fit equation (1 *a*) and (1 *b*). The phase shift between the two curves $I_{up}(\varphi)$ and $I_{down}(\varphi)$ is equal to twice the optical director tilt angle:

$$\delta_{up} - \delta_{down} = 2\theta. \quad (2)$$

At the position of the middle intersection point of the two curves, the two stationary states appear optically equal between crossed polarizers ($I_{up} = \sin^2(2\delta_{up}) = \sin^2(2\delta_{down}) = I_{down}$). The φ-coordinate of this position then corresponds to the angle α between the rubbing direction **x** and the layer normal **k**. The angle α may be equal to the director tilt angle for an ideal horizontal chevron configuration or equal to zero for an ideal vertical chevron configuration.

3. Results

The first series of measurements was taken by slowly heating the oriented sample through the S_C^* phase and recording the $I_{up}(\varphi)$ and $I_{down}(\varphi)$ data for several different temperatures. The data are depicted in figures 4 (*a*)–(*f*) for temperatures $T = 118$, 120, 122, 123, 124 and 125°C, respectively. Filled circles represent the $I_{up}(\varphi)$ and open

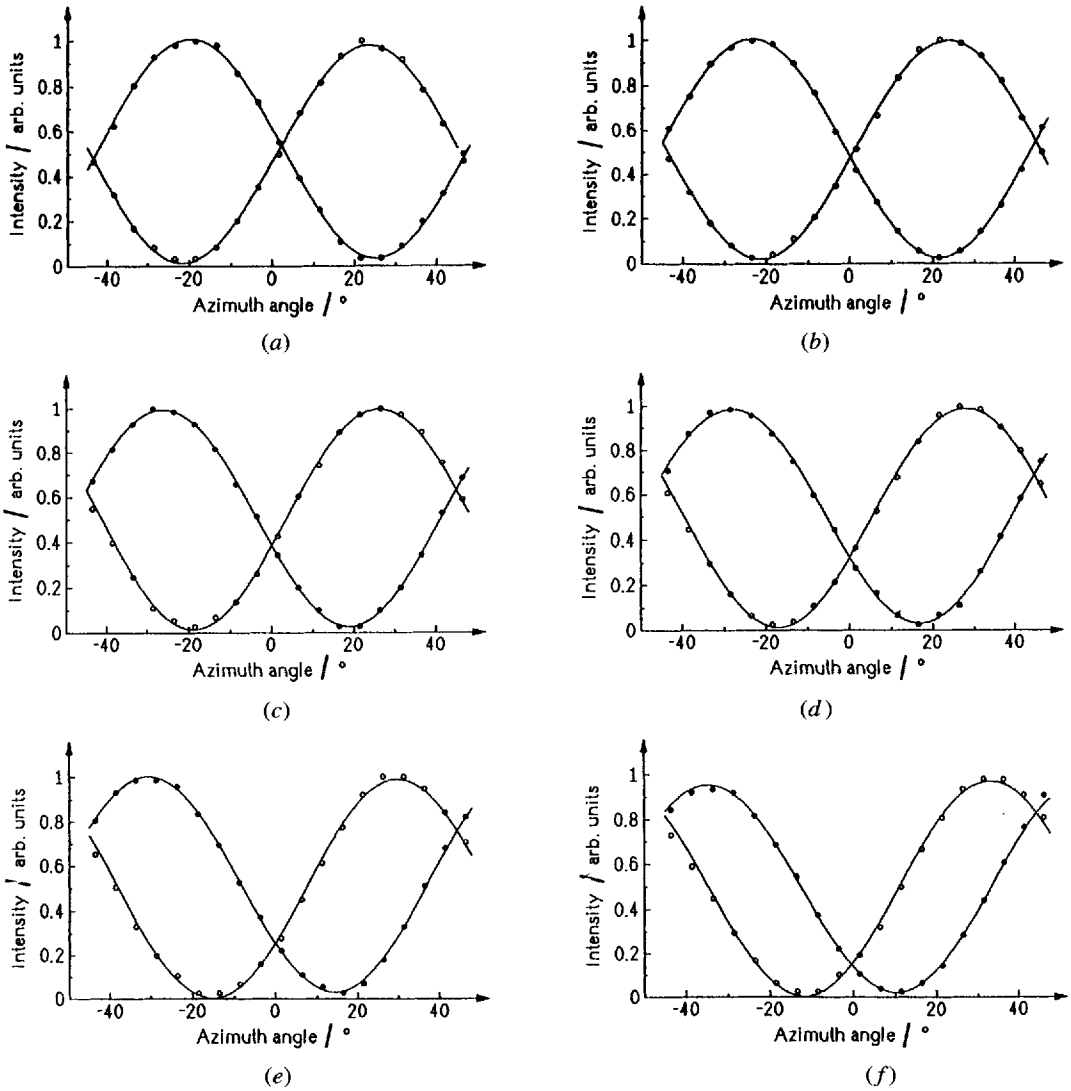

Figure 4. Measurements of the transmitted light intensities of the *polarization up* state (●) and the *polarization down* state (○) as a function of the rotation angle φ of the cell in the plane of the substrate for (*a*) $T = 118$°C, (*b*) $T = 120$°C, (*c*) $T = 122$°C, (*d*) $T = 123$°C, (*e*) $T = 124$°C and (*f*) $T = 125$°C, *before* the high field treatment. Lines depict the results of the best-fit calculations according to equations (1 *a*) and (1 *b*), by means of a simplex algorithm. The middle intersection point of the two curves, which represents the angular position of the layer normal, stays constant at $\varphi = 0$.

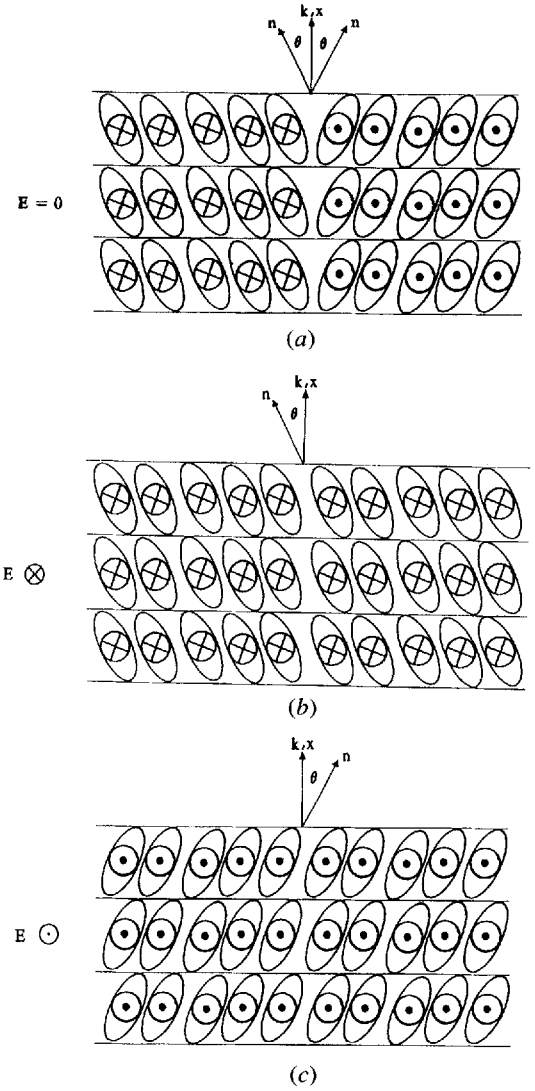

Figure 5. Top view of the layer- and director-configuration in the cell for different directions of the electric field, **E**, *before* the high field treatment. (*a*) **E** = 0, (*b*) **E** in − **z** direction and (*c*) **E** in + **z** direction. **x** is the rubbing direction, **k** the layer normal, **n** the director and θ the director tilt angle.

circles the $I_{down}(\varphi)$ values. The lines are the results of the best-fit calculations, fitting equation (1 *a*) and 1 (*b*) to the normalized data. The phase shift between two respective curves, and therefore the director tilt angle θ, decreases with increasing temperature, as expected. The middle intersection point of the two curves remains constant at $\varphi \approx 0°$, which means that the orientation of the layer normal **k** is independent of temperature and exhibits an angle $\alpha = 0°$ with the rubbing direction **x**, i.e. rubbing direction and projection of the layer normal coincide for all temperatures. This configuration is the well-known *vertical* chevron geometry depicted in figures 5 (*a*)–(*c*) as a top view of the cell. At zero electric field, two kinds of ferroelectric domains are spontaneously formed, one in the polarization 'up' and one in the polarization 'down' state (see figure 5 (*a*)). The angle between the respective directors **n** corresponds to 2θ. Applying an electric field **E** in the − **z** direction, all molecules reorient in the polarization 'down' state and the director **n** makes an angle θ with the layer normal **k** (see figure 5 (*b*)). Reversing the direction of the electric field, the molecules reorient by an angle 2θ along the tilt cone into the polarization 'up' state (see figure 5 (*c*)).

The second series of measurements was obtained after application of a high electric field with amplitude $E = 10\,\mathrm{MV\,m^{-1}}$ at $T = 115°C$ for about 5 s. The $I_{up}(\varphi)$ and $I_{down}(\varphi)$ curves are now considerably different from the respective curves of the first series and are depicted in figures 6 (*a*)–(*f*). The phase shift between two corresponding curves is still the same as before, but the orientation coordinate of the layer normal has changed and is now dependent on temperature. The director tilt angle still has the same value as before (see figure 7), but the angle α between the rubbing direction **x** ($\varphi = 0°$) and the layer normal **k** is now equal to the director tilt angle ($\alpha = \theta$). Figure 8 depicts the dependence of the layer angle α on the director tilt angle θ, parametrized by the temperature. The line shows a least-squares fit, which yields a slope of 1·007, thus giving a functionality $\alpha = \theta$, disregarding the small offset angle $\alpha = 0{\cdot}7°$ for $\theta = 0°$ which is within experimental error for the orientation of the cell in the hot stage.

A structural model for this behaviour is depicted in figure 9 (*a*)–(*c*) and supported by texture photographs (see figures 10 (*a*)–(*c*)), which were taken at a hot stage position $\varphi = 0°$ and temperature $T = 110°C$. After the high field treatment, the director **n** coincides with the rubbing direction **x**. This is only possible, if the layers reorient by an angle $\alpha = \theta$. The director tilt angle θ is essentially fixed by thermodynamics. At zero field after the high field treatment, the two domain types '1' and '2', which have formed, appear equal in intensity and are both in the dark state between crossed polarizers (see figures 9 (*a*) and 10 (*a*)). Applying an electric field in the − **z** direction, molecules of domain type '1', which are in the polarization 'up' state, switch by an angle 2θ into the polarization 'down' state, while the molecules of domain type '2', which are already in the polarization 'down' state, remain in position (see figure 9 (*b*) and figure 10 (*b*)). Reversing the direction of the electric field, all molecules reorient by an angle 2θ and domain type '1' now appears optically as domain type '2' before, and vice versa (see figure 9 (*c*) and 10 (*c*)). Observing the cell between crossed polarizers while applying a low frequency square wave field, the switching between the configurations depicted in figures 9 (*b*) and 9 (*c*) *appears* optically as if the two domain types switch in an opposite fashion (see figures

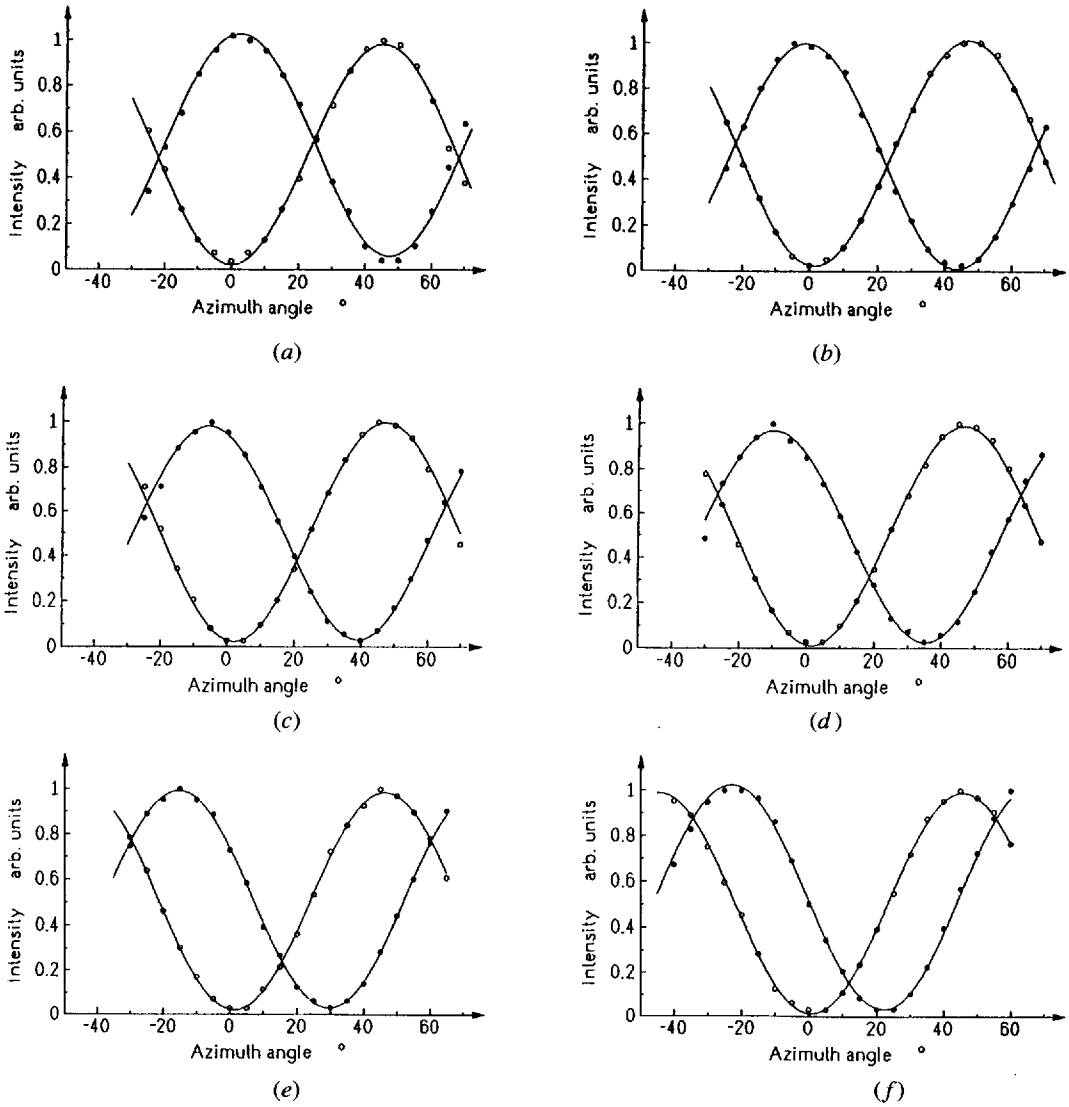

Figure 6. Measurements of the transmitted light intensities of the *polarization up* state (●) and the *polarization down* state (○) as a function of the rotation angle φ of the cell in the plane of the substrate for (*a*) $T = 118°C$, (*b*) $T = 120°C$, (*c*) $T = 122°C$, (*d*) $T = 123°C$, (*e*) $T = 124°C$ and (*f*) $T = 125°C$, *after* the high field treatment. Lines depict the results of the best-fit calculations. The middle intersection point of the two curves, which represents the angular position of the layer normal, now clearly varies as the temperature is changed.

10 (*b*) and 10 (*c*)), due to the different layer orientations for both domain types.

Plotting all curves of the first measurement series (see figures 4 (*a*)–(*f*)) in a single diagram (see figure 11 (*a*)) and those of the second measurement series (see figures 6 (*a*)–(*f*)) in another diagram (figure 11 (*b*)), it is clear that the measurements of the second series were taken in a domain type '2'. Figure 11 (*a*) shows a decreasing director tilt angle with increasing temperature, while the layer normal remains constant at $\varphi = 0°$. This is the well-known process depicted in figure 4, with $\alpha = 0$. Applying the high electric field and reorienting the layers by an angle $\alpha = \theta$, the $I_{down}(\varphi)$ curves coincide for all temperatures, with a minimum light intensity at $\varphi = 0°$, while the $I_{up}(\varphi)$ curves are shifted by the amount of the change of the director tilt angle, when changing the temperature (see figure 11 (*b*)).

The layer configurations of the vertical and horizontal chevron configurations can directly be confirmed by investigation of helical samples of EPHDBPE. This compound also forms horizontal chevrons when exposed to an electric field strength of only $2\,MV\,m^{-1}$. The pitch of the S_C^* helix is about 3 μm, so that preparation of the substance in a 6 μm LC cell produces equidistant disclination lines [1, 2], which are parallel to the layer plane.

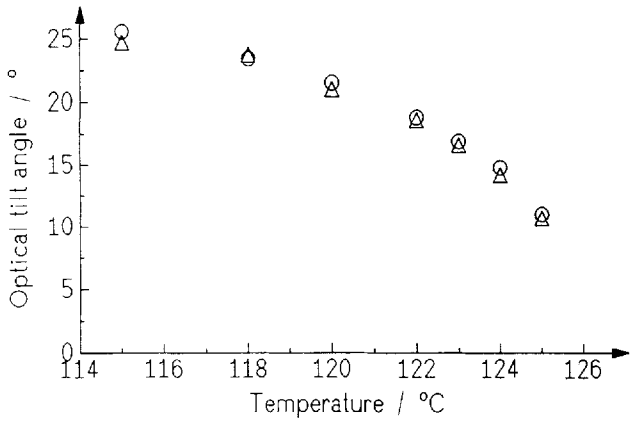

Figure 7. Optical director tilt angle θ as a function of temperature: (○) first measurement series *before* and (△) second measurement series *after* the high field treatment.

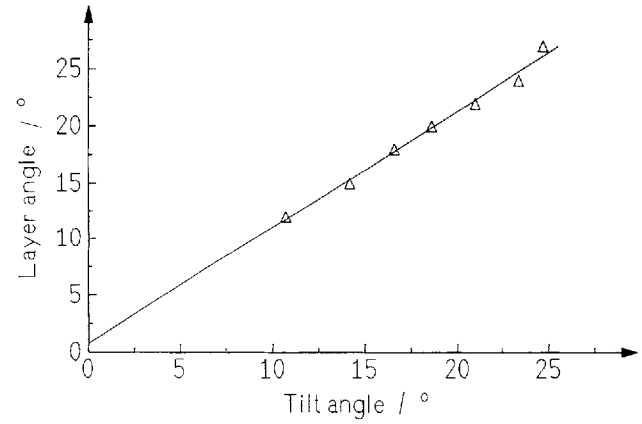

Figure 8. Layer angle α, between the layer normal **k** and the rubbing direction **x**, as a function of the director tilt angle θ. The line represents the result of a linear least-squares fit and yields a slope of 1, which demonstrates the linear relationship $\alpha(T) = \theta(T)$.

Applying a 2 MV m^{-1} electric square field with frequency $f = 200$ Hz for about 5 s produces a domain texture as depicted in figure 12 (*a*) for zero field $E = 0$. Two types of domains are clearly visible. The layers of these domains are tilted in opposite direction with respect to the rubbing direction, as demonstrated by the disclination lines parallel to the layer plane. Application of a positive d.c. field ($E = +1$ MV m^{-1}) or a negative d.c. field ($E = -1$ MV m^{-1}) results in the same observations as discussed above (see figures 12 (*b*) and 12 (*c*), respectively).

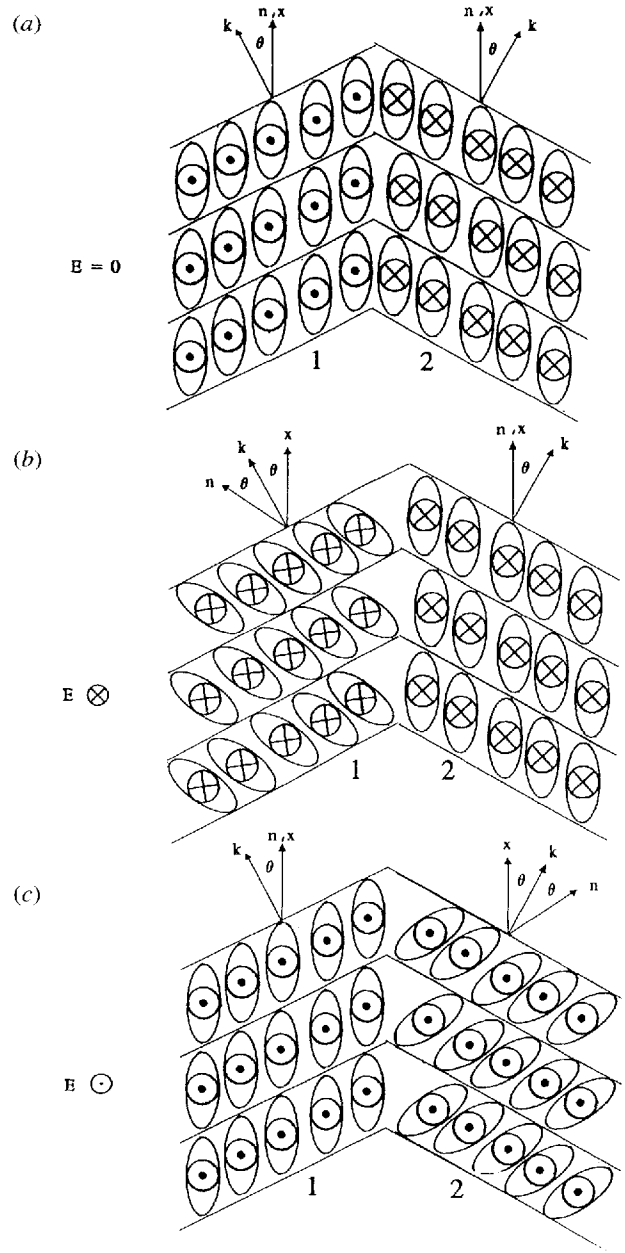

Figure 9. Model of the electric field induced domain structure as a top view of the cell *after* the high field treatment, for different directions of the electric field **E**. (*a*) **E** = 0, (*b*) **E** in − **z** direction and (*c*) **E** in + **z** direction. **x** is the rubbing direction, **k** the layer normal, **n** the director and θ the director tilt angle. The domain types '1' and '2' are the same as those depicted in the texture photographs (see figure 10).

4. Discussion

The field induced domain formation in FLC cells can be explained by a model proposed by Shao *et al.* [19], for the stripe-shaped texture. Recently, several papers have discussed models for the stripe-shaped texture [19–23], and it was usually found that the width of the stripes is approximately equal to the cell gap. The formation of large, field induced domains, which may extend across the whole electrode area of the cell, can be described by an analogous mechanism as proposed in [19].

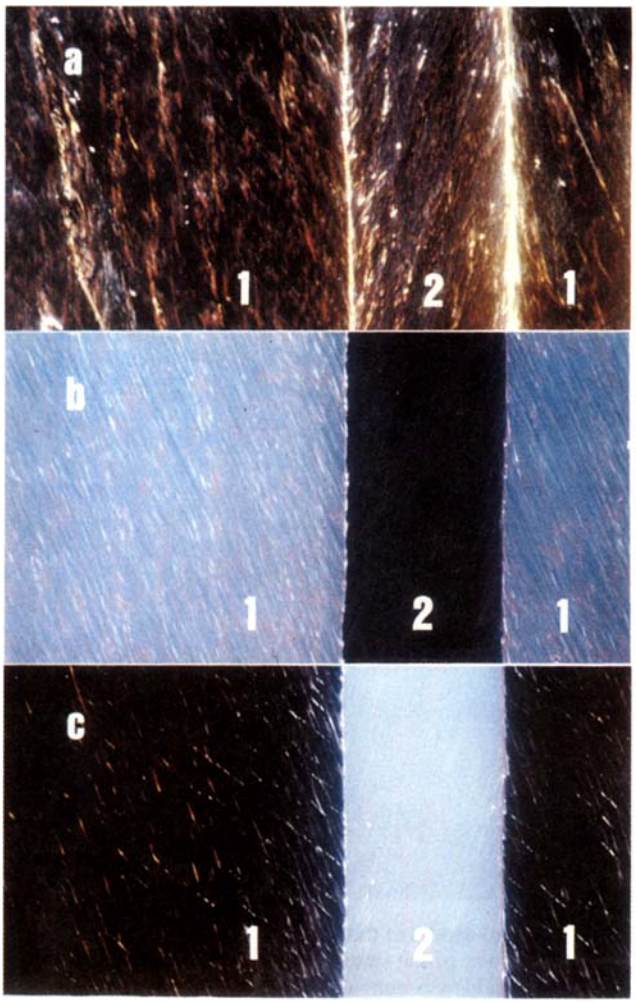

Figure 10. Texture photographs for D8 of the two field induced domain types '1' and '2' *after* the high field treatment. (*a*) $E = 0\,\mathrm{MV\,m^{-1}}$, (*b*) $E = -2\,\mathrm{MV\,m^{-1}}$ d.c. and (*c*) $E = +2\,\mathrm{MV\,m^{-1}}$ d.c. The observed textures are consistent with the model of figure 6. The depicted area is $1 \times 0{\cdot}5\,\mathrm{mm^2}$ in each case.

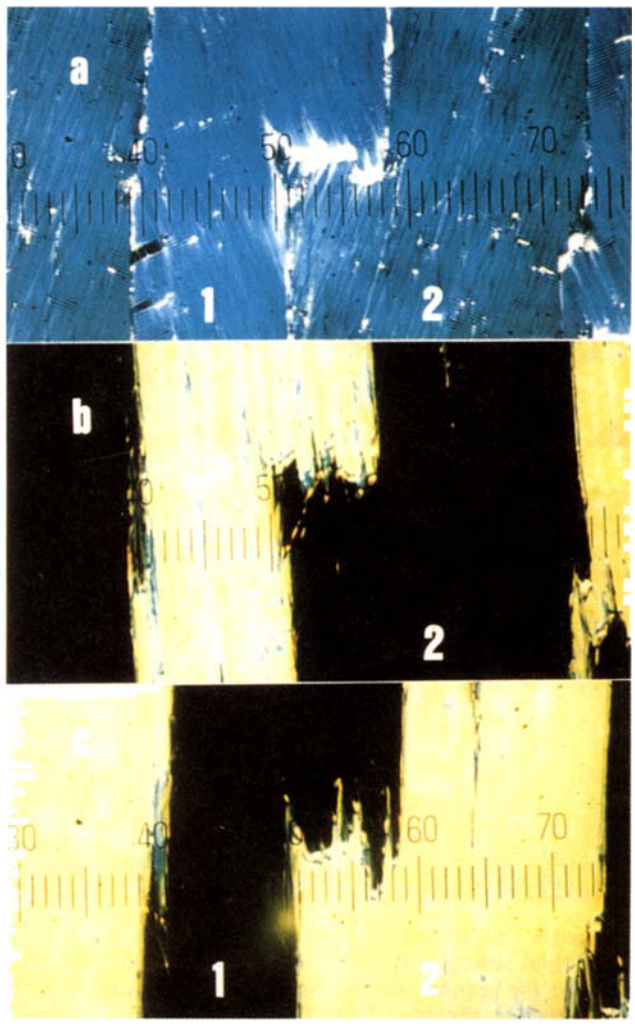

Figure 12. Texture photographs of a helical sample of the compound EPHDBPE *after* the high electric field treatment at $T = 76°C$ (*a*) $E = 0\,\mathrm{MV\,m^{-1}}$; the directions of the layer planes for the two domain types are clearly distinguishable by the disclination lines of the S_C^* helix, (*b*) $E = +1\,\mathrm{MV\,m^{-1}}$ d.c. and (*c*) $E = -1\,\mathrm{MV\,m^{-1}}$ d.c. 10 scale units = 120 μm.

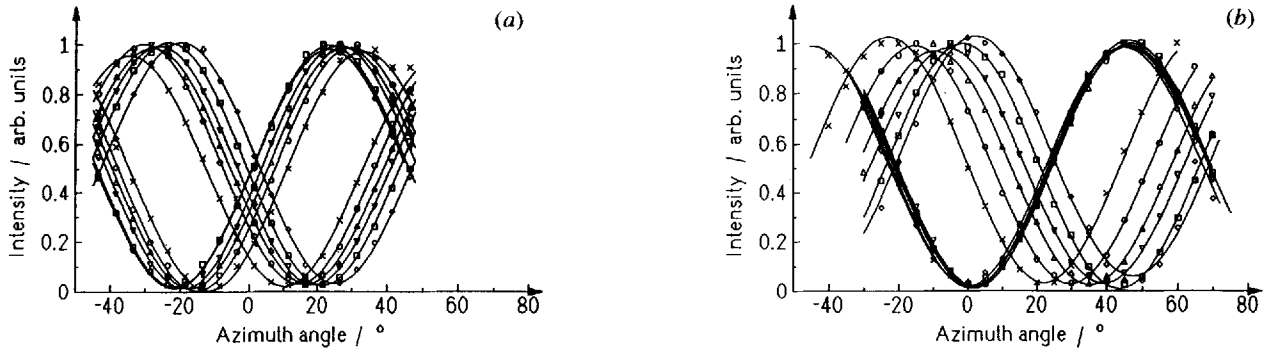

Figure 11. (*a*) The first measurement series *before* the high field treatment, depicted in a single diagram: (◇) $T = 118°C$, (□) $T = 120°C$, (▽) $T = 122°C$, (△) $T = 123°C$, (○) $T = 124°C$ and (×) $T = 125°C$. The phase shift between the $I_{up}(\varphi)$ and $I_{down}(\varphi)$ curves clearly increases with decreasing temperature, accounting for an increase of the director tilt angle, while the middle intersection point of corresponding curves stays constant at $\varphi = 0$, suggesting that the angular position of the layer normal does not change when the temperature is varied. (*b*) The second measurement series *after* the high field treatment, with data point symbols as above. The $I_{down}(\varphi)$ curve stays constant and the $I_{up}(\varphi)$ is shifted to higher values as the temperature is lowered, to account for the increasing director tilt angle. The middle intersection between the two curves, which represents the angular position of the layer normal, now changes when the temperature is varied.

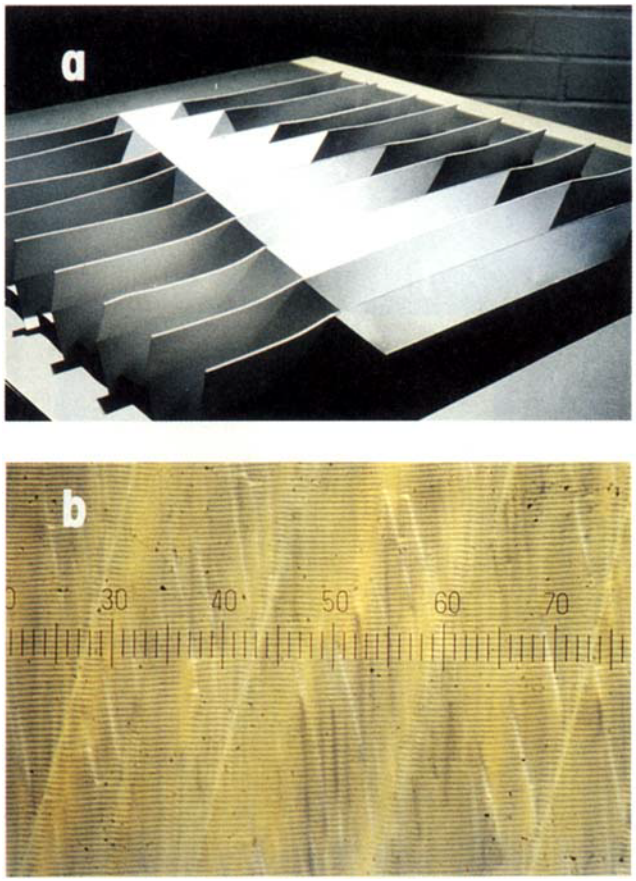

Figure 13. (*a*) Model of the vertical chevron layer structure, the initial structure of the smectic layers in FLC cells, and (*b*) the texture micrograph of a helical sample of this structure, observed for EPHDBPE at $T = 76°C$ *before* the high field treatment. 10 units of scale ≙ 60 μm.

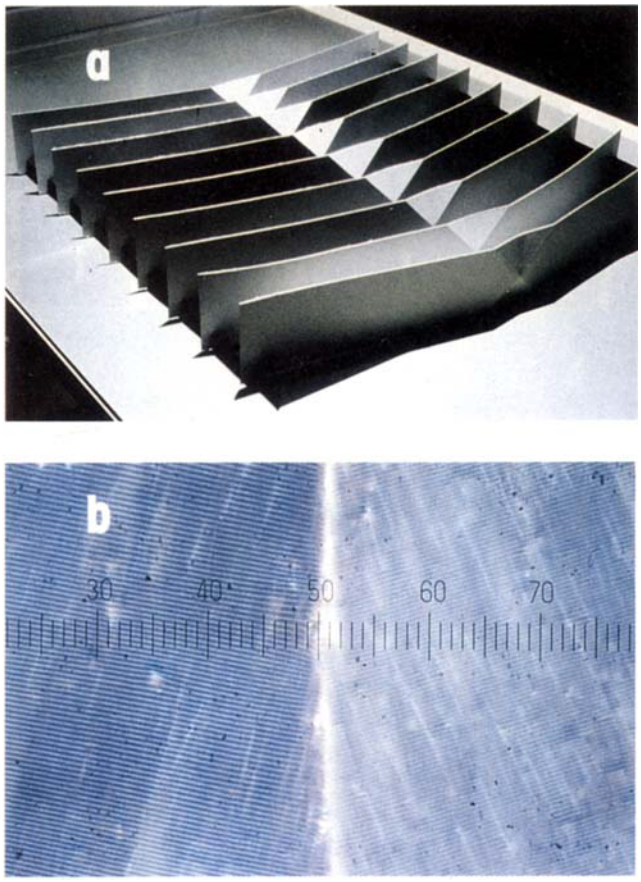

Figure 14. (*a*) Model of the horizontal chevron layer structure, the structure of the smectic layers in the cell *after* the high electric field treatment and (*b*) the texture micrograph of the corresponding helical structure (EPHDBPE, $T = 76°C$, 10 units of scale ≙ 60 μm.)

The initial layer structure in the cell is of the vertical chevron type [4, 5] with zigzag defects mediating regions of chevron shaped layers, tilted in opposite directions [5, 6]. The transition zones are of the bookshelf type with layers tilted by the amount of the chevron angle with respect to the rubbing direction [19]. This structure is depicted in the model of figure 13 (*a*). Figure 13 (*b*) shows a corresponding texture photograph of EPHDBPE with the initially formed, vertical chevron structure. The disclination lines due the S_C^* helix are parallel to the smectic layers and normal to the rubbing direction. The zigzag defects may be discovered by careful observation. The high field treatment forces the chevron layers to straighten up, as has been demonstrated in several publications [24–31]. This means that, by application of a reasonably high electric field, the bookshelf areas, previously mediating two regions of opposite chevron direction, grow at the expense of the chevron regions, until the layer structure in the cell is of bookshelf type with the layer normal inclined to the rubbing direction by the amount of the previous chevron angle. The transition zone between two bookshelf regions of opposite tilt is of the chevron type. The layer structure of the cell now resembles that of the well-established vertical chevron structure turned through 90°, called a horizontal chevron structure, which is depicted in the model of figure 14 (*a*). Figure 14 (*b*) again depicts the corresponding texture photograph of EPHDBPE. The disclination lines due to the S_C^* helix again are parallel to the smectic layers, indicating that the layer configuration has changed as compared to figure 13 (*b*). The chevron transition zone mediating the two field induced domains is clearly observable by its bright colour.

It should be noted that the field induced layer tilt direction can be influenced by an additional small d.c. bias to the applied a.c. electric field as also observed by Patel *et al.* [8, 9]. The time needed for such a reorientation across the whole electrode area is in the order of magnitude of 1–10 s. It should further be noted that the electric field induced domain formation is not restricted to compounds with a N^*–S_C^* transition, where this process is often

observed, but can also appear for compounds with different phase sequences as demonstrated for D8 with a N*–TGB A*–S_A^*–S_C^* sequence.

5. Conclusions

The reorientation of vertical to horizontal chevron configurations in FLC cells for different helical and non-helical samples has been investigated by polarization microscopy and by an electro-optical method, which yields the director tilt angle and the azimuthal position of the smectic layer normal. The layer structure of the cell after a high field treatment resembles that of a horizontal chevron, with the layer normal tilted with respect to the rubbing direction by the amount of the previous chevron angle, which is equal to the director tilt angle for the compound studied. The process of changing the initial vertical chevron structure to the domain structure can be described in terms of a model [19] proposed for the stripe-shaped texture, although there is no relation between the size or shape of the domains and the cell gap, as found for stripe-shaped textures.

The field induced domain formation in FLC cells can be regarded as the transition from a vertical chevron structure, with bookshelf transition zones between regions of opposite chevron direction, to a horizontal chevron structure, with chevron transition zones between bookshelf areas with opposite tilt of the layer normal with respect to the rubbing direction.

This work was supported by a grant from the Deutsche Forschungsgemeinschaft. One of the authors, J.S., is indebted to the Gottlieb Daimler- and Karl Benz-Stiftung for a fellowship. The compound D8 was kindly supplied by Dr J. Kußerow, Institut für Organische Chemie der TU Clausthal.

References

[1] MARTINOT-LAGARDE, PH., 1976, *J. de Phys.*, **37,** C3–129.
[2] MARTINOT-LAGARDE, PH., DUKE, R., and DURAND, G., 1981, *Molec. Crystals liq. Crystals*, **75,** 249.
[3] CLARK, N. A., and LAGERWALL, S. T., 1980, *Appl. Phys. Lett.*, **36,** 899.
[4] RIEKER, T. P., CLARK, N. A., SMITH G. S., PARMAR, D. S., SIROTA, E. B., and SAFINYA, C. R., 1987, *Phys. Rev. Lett.*, **59,** 2658.
[5] CLARK, N. A., and RIEKER, T. P., 1988, *Phys. Rev.* A, **37,** 1053.
[6] OUCHI, Y., TAKANO, H., TAKEZOE, H., and FUKUDA, A., 1988, *Jap. J. appl. Phys.*, **27,** 1.
[7] OUCHI, Y., LEE, J., TAKEZOE, H., FUKUDA, A., KONDO, K., KITAMURA, T., and MUKOH, A., 1988, *Jap. J. appl. Phys. Lett.*, **27,** L725.
[8] PATEL, J. S., and GOODBY, J. W., 1986, *J. appl. Phys.*, **59,** 2355.
[9] PATEL, J. S., SIN-DOO LEE, and GOODBY, J. W., 1989, *Phys. Rev.* A, **40,** 2854.
[10] ANDERSSON, G., FLATISCHLER, K., KOMITOV, L., LAGERWALL, S. T., SKARP, K., and STEBLER, B., 1991, *Ferroelectrics*, **113,** 361.
[11] SKARP, K., ANDERSSON, T., HIRAI, T., YOSHIZAWA, A., HIRAOKA, K., TAKEZOE, H., and FUKUDA, A., 1992, *Jap. J. appl. Phys.*, **31,** 1409.
[12] WALBA, D. M., VOHRA, R. T., CLARK, N. A., HANDSCHY, M. A., XUE, J., PARMA, D. S., LAGERWALL, S. T., and SKARP, K., 1986, *J. Am. chem. Soc.*, **108,** 7424.
[13] The epoxide is available from Aldrich Chemicals.
[14] DIERKING, I., GIEßELMANN, F., ZUGENMAIER, P., KUCZYNSKI, W., LAGERWALL, S. T., and STEBLER, B., 1993, *Liq. Crystals*, **13,** 45.
[15] NGUYEN, H. T., BABEAU, A., LÉON, C., MARCEROU, J.-P., DESTRADE, C., SOLDERA, A., GUILLON, D., and SKOULIOS, A., 1991, *Liq. Crystals*, **9,** 253.
[16] DIERKING, I., GIEßELMANN, F., and ZUGENMAIER, P., 1994, *Liq. Crystals*, **17,** 17.
[17] DIERKING, I., GIEßELMANN, F., KUßEROW, J., and ZUGENMAIER, P., 1994, *Liq. Crystals*, **17,** 243.
[18] BAHR, CH., and HEPPKE, G., 1987, *Liq. Crystals*, **2,** 825.
[19] SHAO, R. F., WILLIS, P. C., and CLARK, N. A., 1991, *Ferroelectrics*, **121,** 127.
[20] LEJCEK, L., and PIRKL, S., 1990, *Liq. Crystals*, **8,** 871.
[21] FÜNFSCHILLING, J., and SCHADT, M., 1991, *Jap. J. appl. Phys.*, **30,** 741.
[22] JAKLI, A., and SAUPE, A., 1992, *Phys. Rev.* A, **45,** 5674.
[23] ASAO, Y., and UCHIDA, T., 1993, *Jap. J. appl. Phys. Lett.*, **32,** L604.
[24] HARTMANN, W., 1988, *Ferroelectrics*, **85,** 67.
[25] JOHNO, M., CHANDANI, A. D. L., OUCHI, Y., TAKEZOE, H., FUKUDA, A., ICHIHASHI, M., and FURUKAWA, K., 1989, *Jap. J. appl. Phys. Lett.*, **28,** L119.
[26] SATO, Y., TANAKA, T., KOBAYASHI, H., AOKI, K., WATANABE, H., TAKESHITA, H., OUCHI, Y., TAKEZOE, H., and FUKUDA, A., 1989, *Jap. J. appl. Phys. Lett.*, **28,** L483.
[27] UCHIDA, T., HIRANO, M., and SAKAI, H., 1989, *Liq. Crystals*, **5,** 1127.
[28] HARTMANN, W., and LUYCKX-SMOLDERS, A. M. M., 1990, *J. appl. Phys.*, **67,** 1253.
[29] ITOH, K., JOHNO, M., TAKANISHI, Y., OUCHI, Y., TAKEZOE, H., and FUKUDA, A., 1991, *Jap. J. appl. Phys.*, **30,** 735.
[30] OH-E, O., ISOGAI, M., and KITAMURA, T., 1992, *Liq. Crystals*, **11,** 101.
[31] GIEßELMANN, F., and ZUGENMAIER, P., 1993, *Molec. Crystals liq. Crystals*, **237,** 121.